UNIVERSIDAD TECNOLÓGICA METROPOLITANA del Estado de Chile
UTEM

https://revistammsb.utem.cl | revista.mmsb@utem.cl
ISSN-L: 2735-6817 | ISSN (online): 2735-6817

REVISTA MMSB
Revista de Modelamiento Matemático de Sistemas Biológicos
Vol.3(2023), No.E, pp.1–14, e23R05
https://doi.org/10.58560/rmmsb.v03.n02.023.04

Using the Chemical Master Equation to model the interaction network of focal adhesion proteins

Utilizando la Ecuación Maestra Química para modelar la red de interacción de las proteínas de adhesión focal.

Luciana Renata de Oliveira[1], Júlia Vitória Ribeiro[1] Alícia Groth Becker[1], Gabriel Vitorello[1] and José Carlos Merino Mombach[1]

✉ Luciana Renata de Oliveira: lucianarenatadeoliveira@gmail.com

[1] Departamento de Física, Centro de Ciências Naturais e Exatas,
Universiade Federal de Santa Maria,
Santa Maria, RS, Brasil

Recepción: 2023-06-01 | Aceptación: 2023-09-10 | Publicación: 2023-10-29

Recommended Citation: Renata de Oliveira, L. *et al.* (2023). *'Using the Chemical Master Equation to model the interaction network of focal adhesion proteins'*. Rev. model. mat. sist. biol. 3(E), e23R05, doi:10.58560/rmmsb.v03.n02.023.04

Support: PIBIC No. 21-2022, PROA 23-25551-0001199-9 (2023)

ABSTRACT

Cells are exposed to mechanical stresses, whether through external forces that are applied to tissues or endogenous forces that are generated within the active cytoskeleton. The differences in the stimuli are sensed by cells and controlled by a network of focal adhesion proteins that regulate signaling pathways and determine cellular responses including cell motility, proliferation, and cell differentiation (cell fate). Together the ability of cells to sense and respond to mechanical stimuli governed by mechanosensors and mechanosignaling proteins can be termed mechanotransduction. Whilst there is intense ongoing research on specific pathways involved in mechanoresponse mechanisms, the experiments alone can only give a global overview of dynamic parameters for the interaction of proteins. The focal adhesion pathway is a complex network and the use of stochastic mathematical algorithms can be an efficient tool to expand and explore this network by building and solving a regulatory interaction map. Exploring the predicted interaction networks can suggest new directions for future experimental research and provide cross-species predictions for efficient interaction mapping. Here we aim to describe the network representing a subset of proteins associated with focal adhesion using the stochastic model Chemical Master Equation and shed further light on how the dynamic of these proteins can directs cell behavior and responses. Our results showed that our model is able to describe the experimental interactions. In addition, it is able to model the temporal cascade of events related to responses to mechanical stimuli and showed different dynamical behaviors based on the kinetic parameters.

Keywords:

Chemical Master equation, Focal Adhesion, Signaling Networks, Stochastic Model

RESUMEN

Las células están expuestas a tensiones mecánicas, ya sea a través de fuerzas externas aplicadas a los tejidos o fuerzas endógenas generadas dentro del citoesqueleto activo. Las diferencias en los estímulos son percibidas por las células y controladas por una red de proteínas de adhesión focal que regulan las vías de señalización y determinan respuestas celulares, incluida la movilidad celular, la proliferación y la diferenciación celular (destino celular). En conjunto, la capacidad de las células para percibir y responder a estímulos mecánicos, gobernada por mecanosensores y proteínas de señalización mecánica, puede denominarse mecanotransducción. Si bien hay una intensa investigación en curso sobre las vías específicas involucradas en los mecanismos de respuesta mecánica, los experimentos por sí solos solo pueden proporcionar una visión general de los parámetros dinámicos para la interacción de las proteínas. La vía de adhesión focal es una red compleja y el uso de algoritmos matemáticos estocásticos puede ser una herramienta eficiente para expandir y explorar esta red mediante la construcción y resolución de un mapa de interacción reguladora. La exploración de las redes de interacción predichas puede sugerir nuevas direcciones para futuras investigaciones experimentales y proporcionar predicciones entre especies para mapeos de interacción eficientes. Aquí nuestro objetivo es describir la red que representa un subconjunto de proteínas asociadas a la adhesión focal utilizando el modelo estocástico de la Ecuación Maestra Química y arrojar más luz sobre cómo la dinámica de estas proteínas puede dirigir el comportamiento y las respuestas celulares. Nuestros resultados mostraron que nuestro modelo es capaz de describir las interacciones experimentales. Además, puede modelar la cascada temporal de eventos relacionados con respuestas a estímulos mecánicos y mostró diferentes comportamientos dinámicos basados en los parámetros cinéticos.

Palabras Claves:

Ecuación Maestra Química, Adhesión Focal, Redes de Señalización, Modelo Estocástico

2020 AMS Mathematics Subject Classification: Primary: 92B05; Secondary: 104A54, 104A62

1 INTRODUCTION

Human anatomy consists of various types of tissues, ranging from the very soft gyri and sulci of the brain to the very hard rigid trabeculae of bones Atherton *et al.* (2016). In our tissues, cells experience numerous mechanical stimuli, for example, shear stresses from the blood flow or stretching and compression forces from several tissues associated with muscle activity Jansen *et al.* (2017). Adherent cells respond very sensitively not only to biochemical but also to the physical properties of their environment. For example, it has been shown that stem cell differentiation can be guided by substrate rigidity, which is sensed by cells by actively pulling on their environment with actomyosin-generated forces Roca-Cusachs *et al.* (2013). Force, therefore, plays an important role in the shaping, development, and maintenance of tissues and organs. Virtually all organisms have evolved structures from the macroscale (organs, tissues) to the microscale (cells) and nanoscale (molecular assemblies, single proteins) that are sensitive and responsive to myriad forces, including compressive, tensile, shear stress, and hydrostatic pressure Jansen *et al.* (2017); Atherton *et al.* (2016); Roca-Cusachs *et al.* (2013).

The ability of cells to sense and respond to mechanical stimuli is termed mechanotransduction Kanchanawong *et al.* (2010), including not only all components of force, stress, and strain but also substrate rigidity, topology, and adhesiveness. This ability is crucial for the cell to respond to the surrounding mechanical cues and adapt to the changing environment Nagano *et al.* (2012); Del Rio *et al.* (2009). Cells sense their microenvironment using a variety of receptors. Integrins are one of the most prominent receptor families that bind proteins of the extracellular matrix (ECM), which consist of fibrous protein filaments that are organized in aligned fibers (e.g. co-aligned fibers in forming tendons) or highly organized membranous networks (e.g. the basement membranes underneath of epithelial cell layers). The organization, the biochemistry, and the mechanical properties of integrins depend on the type of ECM proteins they are assembled with. With their intracellular domains, integrins associate with a large number of proteins (focal adhesion plaque proteins) that link them to the contractile actomyosin cytoskeleton Hirata *et al.* (2014); Roca-Cusachs *et al.* (2013); Nagano *et al.* (2012). These multiprotein complexes appear as focused adhesion structures when observed under the fluorescence microscope and hence are called focal adhesions (FAs) (Figure 1) Atherton *et al.* (2016); Jansen *et al.* (2017); Roca-Cusachs *et al.* (2013); Nagano *et al.* (2012).

Upon binding to ECM integrins become activated and form initial clusters at the cell membrane. Mechanical forces can support the integrin activation process involving conformational changes of the receptor that promotes not only high-affinity interaction with the ECM but also induces the recruitment of a number of proteins to the intracellular integrin cytoplasmic domain. Two of the critical proteins that connect integrins with the actin cytoskeleton are the adapter proteins talin and vinculin. Because of the key role sensing of their mechanical environment, talin and vinculin are often described as mechanosensors and they have multiple binding sites for other proteins. Talin for example, in addition to vinculin, binds to the focal adhesion kinase (*FAK*), paxillin, RIAM, DLC1, actin, and others Hirata *et al.* (2014); Kumar *et al.* (2016); vinculin binds to ponsin, vinexin (a+b), CAP, Arp/2/3, paxillin, and actin Carisey *et al.* (2013); Del Rio *et al.* (2009); Chen *et al.* (2006). Some of these proteins, i.e. *FAK* and paxillin together with the *SRC* kinase trigger signaling pathways that regulate downstream the family of RhoGTPAses, a protein family that governs actin polymerization (i.e. through Rac1) and/or myosin-mediated actin bundling and contraction (i.e. *RhoA*). The latter group of proteins can thus be regarded as mechanosignalling proteins that translate the mechanosensory information into chemical signals that coordinate specific cellular responses.

There are many other proteins besides those mentioned above that contribute to mechanotransduction (Figure 1). In fact, mass spectroscopy experiments have identified more than 2,000 proteins and around 60 of them belong to the core adhesion proteins that are directly involved in cell-matrix adhesion regulation Kanchanawong *et al.* (2010); Atherton *et al.* (2016); Hirata *et al.* (2014); Roca-Cusachs *et al.* (2013); Chen *et al.* (2006). How they work together and coordinate the process of cell-matrix communication is yet unclear.

The trove of quantitative data produced by modern biology has highlighted that the complex behaviors of biological systems, even the simplest ones, are difficult to comprehend with experiments alone De Oliveira (2014). These systems are not isolated, but rather subject to intrinsic and extrinsic fluctuations, which leads to a quasi-equilibrium state (homeostasis) Van Kampen (1992); De Oliveira (2014); Aguda and Friedman (2008). An increasing number of experimentalists appreciate the need for mathematical modeling to explain their data and uncover the underlying molecular mechanisms for their biological systems Berro (2018).

As illustrated in Figure 1 the focal adhesion pathway is a complex network and the use of stochastic mathematical algorithms can be an efficient tool to expand and explore this network by building and solving a regulatory interaction map. Protein-protein interaction networks are an important ingredient for the system-level understanding of cellular processes. Exploring the predicted interaction networks can suggest new directions for future experimental research and provide cross-species predictions for efficient interaction mapping.

Here we propose using the Chemical Master Equation to understand the dynamic interactions between proteins in the focal adhesion. We specifically show how the biochemical network involving extracellular matrix stimuli can lead to actin polymerization and focal adhesion formation. Next we present the detailed methodology to build the biochemical network and how to build the stochastic model.

doi: 10.58560/rmmsb.v03.n02.023.04

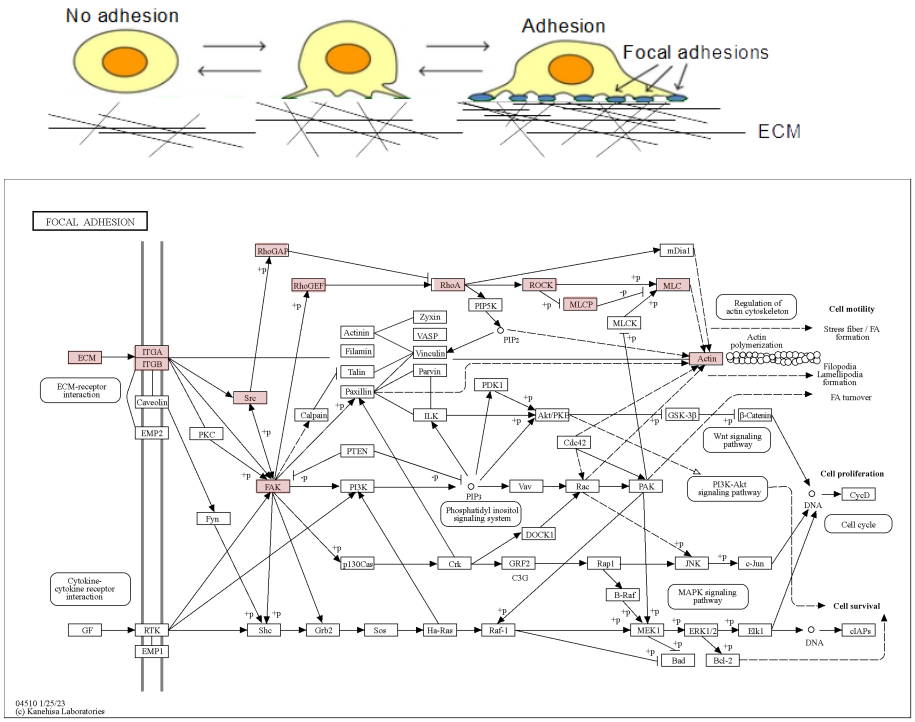

Figure 1: Top: Schematic representation of focal adhesion formation. Botton: Signaling pathway map for focal adhesion proteins. This figure is a reproduction of the network generated by the Kyoto Encyclopedia of Genes and Genomes (KEGG) (https://www.genome.jp/pathway/map04510) for focal adhesion. The proteins modeled in this paper are highlighted.

2 METHODOLOGY

SIGNALING NETWORK FOR FOCAL ADHESION PROTEINS

We built a signaling network considering the interaction between the focal adhesion proteins *FAK*, *SRC*, Rac, Rho, Myosin light-chain (*MLC*), that leads to actin polymerization and focal adhesion formation (Figures 1 and 2). We choose specifically these proteins because they are involved in many important cellular processes, including health and disease. *FAK*-*SRC* interaction is crucial for the initiation and regulation of focal adhesions Roca-Cusachs *et al.* (2013). Furthermore, *FAK*, plays a role in promoting growth factor– and integrin-stimulated cell motility in both normal and transformed cells and increased *FAK* expression are connected with elevated tumorigenesis Hsia *et al.* (2003). *SRC* activity has a role in normal vascular smooth muscle contractile function and in vascular remodeling in cardiovascular disease MacKay and Knock (2015). Rho/ROCK pathway is involved in synapses in pathological situations such as spinal cord injury/ischemia, Alzheimer's disease, Parkinson's disease, multiple sclerosis, amyotrophic lateral sclerosis (ALS), and spinal muscular atrophy (SMA) Martin-Camara *et al.* (2021). And abnormal activation of Rho kinase signaling is closely associated with major cardiovascular diseases such as systemic hypertension, pulmonary hypertension, vasospasm, and adverse cardiac remodeling Dai *et al.* (2018).

In our study, the signaling network of proteins and their interactions are constructed based on published data, the Kyoto Encyclopedia of Genes and Genomes (KEGG) database and the database for protein-protein interactions Search Tool for the Retrieval of Interacting Genes/Proteins (STRING) Szklarczyk *et al.* (2019). In our model, each state of the proteins is considered as one component of the network (for example *FAK* protein (*FAK*) and *FAK* phosphorylated ($p-FAK$), Figure 2). Multiple types of interactions are taken into account, both positive (activation, phosphorylation) and negative (inhibition).

Our model is composed of three circuits (Figures 1 and 2): The initial activation by the extracellular matrix and the membrane protein Integrin [8-14] which activates both *FAK* and *SRC*. *FAK* and *SRC* form a positive feedback loop Caron-Lormier and Berry (2005). *FAK* and *SRC* are connected with the second circuit, the Rho family, *FAK* activates *RhoGEF* and *SRC* activates *RhoGAP*. *RhoGAP* inhibits and *RhoGEF* activates *RhoA* Pertz (2010). *RhoA* indirectly activates *MLC* Lessey *et al.* (2012). The cell fate is actin polymerization that will lead to focal adhesion formation Soriano *et al.* (2021). Valencia-Expósito et. al Valencia-Expósito *et al.* (2016) proved that actomyosin contractility is controlled primarily by reversible phosphorylation of the myosin-II regulatory light chain (*MLC*) through the action of myosin kinases and phosphatases. Their results demonstrate that actomyosin oscillations in which the combination of cooperative binding of actin filaments in conjunction with actin filament dissociation from the bundle, due to myosin-induced tension, is sufficient to generate cell-autonomous oscillations in myosin and F-actin content. With these results here we are

associating the behavior of *MLC* with the actin, which is the output of the model. This signaling network is used to build the stochastic mathematical model as presented in the next section.

MATHEMATICAL MODEL FOR PROTEIN INTERACTIONS

In biochemistry, Michaelis–Menten kinetics is the simplest case of enzyme kinetics, applied to enzyme-catalysed reactions of one substrate and one product Srinivasan (2022). It takes the form of an equation describing the rate reaction rate v (rate of formation of product P, with concentration $[P]$) to $[S]$, the concentration of the substrate S Its formula is given by the Michaelis–Menten equation:

$$v = \frac{dp}{dt} = \frac{k_{SP}[S][P]}{K_m + [P]} \tag{1}$$

where $V = k_{SP}[S]$ represents the limiting rate approached by the system at saturating substrate concentration for a given enzyme concentration. When the value of the Michaelis constant K_m is numerically equal to the substrate concentration, the reaction rate is half of V Raaijmakers (1987).
This kind of approach can be used to model protein-protein interactions as we are interested in this paper. To illustrate how to build the system with differential equations to describe the interactions we brought three kinds of examples in Figure 3. Let's consider that we have two types of proteins A and B, which can interact as represented in Figure 3. For our network, we can represent the interactions as (1) $A \rightarrow B$, where protein A activates protein B, such a process can be represented by a Michaelis-Menten reaction equation. The concentration of protein B, which is represented as $[B]$ increases as the product of protein A and the transition rate of activation of B by A that is represented by k_{AB} in Table 1. (2) $B \rightarrow A$ represents the Degradation of protein B to A with a rate k_{BA} in Table 1. (3)$A \dashv B$ represents the inhibition of B due to A. This dynamic interaction is also represented by a Michaelis-Menten equation such as represented in Table 1.

Taking the interactions for our network in Figure 2, we have the equations corresponding to each interaction in Table 1 in the Appendix. With these equations representing the interactions, we can build a system of differential equations to study the time evolution of the network in Figure 2, as follows.

Table 1: List of equations for each reaction represented in Figure 3.

Reaction	Equation	Reaction kind
$A \rightarrow B$	$\frac{k_{AB}[A][B]}{k_j+[B]}$	Activation
$B \rightarrow A$	$k_{BA}[B]$	Degradation
$A \dashv B$	$\frac{k_{AB}[A][B]}{k_j+[B]}$	Inhibition

$$\frac{d[FAK^p]}{dt} = \frac{k_{EF^p}([ECMINT]-[p-MLC])[FAK]}{k_1+[FAK]} + \frac{k_{FF^p}[FAK][p-FAK]}{k_3+[p-FAK]} + \frac{k_{S^pF^p}[p-SRC][FAK]}{k_7+[FAK]} + - k_{F^pF}[p-FAK] - \frac{k_{F^pS^p}[p-FAK][SRC]}{k_4+[SRC]} + - \frac{k_{F^pRhoGEF}[p-FAK][RhoGEF]}{k_8+[RhoGEF]}$$

$$\frac{d[SRC^p]}{dt} = \frac{k_{ES^p}([ECMINT]-[p-MLC])[SRC]}{k_2+[SRC]} + + \frac{k_{F^pS^p}[p-FAK][SRC]}{k_4+[SRC]} + \frac{k_{SS^p}[SRC][p-SRC]}{k_6+[p-SRC]} - k_{S^pS}[p-SRC] + - \frac{k_{S^pF^p}[p-SRC][FAK]}{k_7-[FAK]} + \frac{k_{S^pRhoGAP}[p-SRC][RhoGAP]}{k_9+[RhoGAP]}$$

$$\frac{d[RhoGEF]}{dt} = \frac{k_{F^pRhoGEF}[p-FAK][RhoGEF]}{k_8+[RhoGEF]} + - \frac{k_{RhoGEFRhoA}[RhoGEF][RhoA]}{k_{10}+[RhoA]}$$

$$\frac{d[RhoGAP]}{dt} = \frac{k_{S^pRhoGAP}[p-SRC][RhoGAP]}{k_9+[RhoGAP]} + - \frac{k_{RhoGAPRhoA}[RhoGAP][RhoA]}{k_{11}+[RhoA]}$$

$$\frac{d[RhoA]}{dt} = \frac{k_{RhoGEFRhoA}[RhoGEF][RhoA]}{k_{10}+[RhoA]} + - \frac{k_{RhoGAPRhoA}[RhoGAP][RhoA]}{k_{11}+[RhoA]}$$

$$\frac{d[p-MLC]}{dt} = \frac{k_{RHOAMLC^p}[RhoA]][MLC]}{k_{12}+[MLC]} + + \frac{k_{MLCPMLC^p}[MLC][p-MLC]}{k_{13}+[MLC]} - k_{MLC^pMLC}[p-MLC]$$

The term $[ECMINT]-[p-MLC]$ in the equations represents the negative feedback that the actin polymerization will send to the extracellular matrix. In nature, the signal is not continuous and stops once the actin polymerization starts and it is represented by the balance between the extracellular matrix concentration $[ECM]$ and the actin signal $[p-MLC]$ Atherton *et al.* (2016).
We are assuming the conservation of proteins and the concentrations of inactive *FAK*, *SRC*, and *MLC* can be derived from the total number of molecules and the number of phosphorylated proteins. Next, we discuss how to build the stochastic model from the differential equations.

doi: 10.58560/rmmsb.v03.n02.023.04

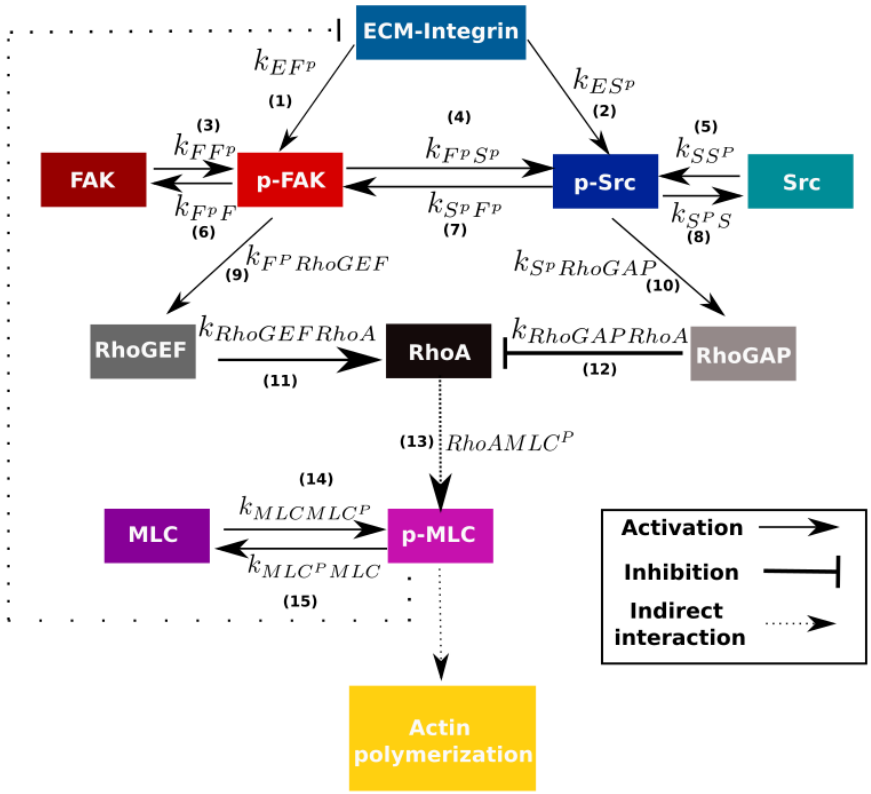

Figure 2: Network considering the pathway of proteins involved in the ECM mediated mechanosensing leading to actin polymerization. The numbers correspond to the equations in Table 1.

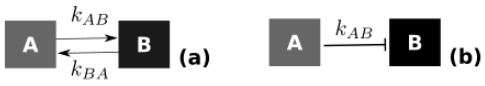

Figure 3: Mathematical representation of a biochemical network. (a) Activation and degradation of proteins. (b) Inhibition of proteins.

CHEMICAL MASTER EQUATION FOR THE DESCRIPTION OF PROTEIN MECHANOSIGNALING

The Chemical Master Equation is a class of discrete-state, continuous-time Markov processes that describe the time evolution of a system that can be modeled as a probabilistic combination of states Van Kampen (1992). For the mechanosignaling network (Figure 2) the states are represented by the concentration of proteins in inactive, or active states usually determined by phosphorylation and/or conformational changes. The concentration of proteins is modeled as temporal variables assuming positive values represented by $[protein]$, that is the number of individuals in each protein state, for example, the number of molecules in inactive *FAK* ($[FAK]$) or phosphorylated *FAK* ($[p-FAK]$). The time evolution of the variable's concentrations is modeled by rates representing their interactions, where activation rates represent the interactions for which there is an increase in the protein concentration, for example, the increment in the concentration of phosphorylated *SRC* ($[p-SRC]$) due to k_{ss^p} and the inhibition rates represent the interactions for which there is a decrease in the concentration of the protein, for example in the dephosphorylation of phosphorylated *MLC* ($[p-MLC]$) due to k_{MLC^pMLC} (Figure 2). It is important to note that the system of equations describes one protein concentration in correspondence with the concentration of the others Van Kampen (1992); De Oliveira (2014). The chemical master equation for the system is written as

$$\begin{aligned}\frac{\mathrm{d}p([protein])}{\mathrm{d}t} &= r([protein]+1,t)p([protein]+1,t)+\\ &+g([protein]-1,t)p([protein]-1,t)+\\ &-(r(n_{protein},t)+g(n_{protein},t))p(n_{protein},t)\end{aligned} \tag{2}$$

Where each protein is represented by a combination of the gain term ($g([protein],t)$) responsible for the increment of the concentration of the protein ($[protein]$ to $[protein]+1$) and the recombination term ($r([protein],t)$) responsible for the decrease of the concentration of the protein ($[protein]$ to $[protein]-1$), the generation and recombination of each protein are described in Table 2. $p([protein],t)$ is the occupation probability per unit of time of a determined state in the system. In our case, it is represented by the concentra-

tion of a protein. The generation and recombination terms used to build the stochastic model using the chemical master equation for each reaction in our network (Figure 2) are represented in Table 2.

3 RESULTS: SOLUTION OF THE PATHWAY LEADING TO ACTIN POLYMERIZATION

Here we are interested in exploring the signaling network of focal adhesion proteins leading to actin polymerization and focal adhesion formation (Figures 1 and 2) to illustrate the use of stochastic models such as the Chemical Master Equation for the understanding of protein interactions leading to different cell fates. The network was built considering the interaction between the focal adhesion proteins (see Section 2) and the solution for the dynamic interactions of the proteins is given by the solution of the Chemical Master Equation (Eq. 2) with the corresponding generation and recombination terms (as shown in Section 2). The output of this model is the dynamic interactions of proteins, which can be seen as the distribution of molecules in each protein state per time (Figure 4). The system of equations is solved numerically using the Gillespie algorithm Giampieri *et al.* (2011); Gillespie (1977). The input parameters are the initial distribution of proteins, the total time of simulation, and the values of the transition rates (see Tables 3 and 4 for details). Experiments alone cannot give exactly the values of protein concentration or transition rates, because the methodologies used to describe protein dynamics such as Fluorescence recovery after photobleaching (FRAP) or single molecule tracking follows one protein at a time and only tag a sub-population of proteins due to diffraction effects de Oliveira and Jaqaman (2019); Jaqaman *et al.* (2008); Lippincott-Schwartz *et al.* (2018). But we used experimental data to estimate the range of transition rate values and initial protein concentration used in the simulations Carisey *et al.* (2013); Caron-Lormier and Berry (2005); Calderwood *et al.* (2013); Stutchbury *et al.* (2017).

In Figure 4 we show the results for Case 1 in Tables 3 and 4. We can see that $p-FAK$ and $p-SRC$ are the first to be activated, followed by the Rho family and later by MLC and $p-MLC$ (Figure 4a). This cascade effect behaves as expected by the construction of the model and the experimental information we had about the system. The higher values of the transition rates k_{EF^p}, k_{ES^p} and k_{FF^p} were chosen to guarantee that these reactions would happen often and coordinate all the other events. In Figure 4b we have the detailed behavior for all 4 circuits in our model. The results showed that the activity of *FAK* and $p-FAK$ occurs only at the beginning of the process (Figure 4b(i)) and $p-FAK$ reached its peak activity at around 30 MCS. SRC and $p-SRC$ continue to be activated longer in simulation (Figure 4b(ii)), and $p-SRC$ achieved its peak at around 1300MCS. Another interesting behavior we can observe for $p-SRC$ is that it has other peaks later in time, meaning that it is activated in waves. The activation of *RhoGAP* and $RhoGEF$ (peaks at around 2600 MCS and around 120 MCS respectively) leads to the activation of *RhoA*, with maximum activity at around 1500 MCS. The circuit MLC-pMLC increased its activity later on reaching its peak at around 3500 MCS for $p-MLC$. The concentration of MLC goes to zero when the $p-MLC$ reaches its stability. This behavior is occurring because MLC is not regulated by any other protein and its role is to activate $p-SRC$. Once $p-SRC$ is activated the protein degrades. It is interesting to notice that the sequence of events is: activation of $p-FAK$ followed by activation of $RhoGEF$, then $p-SRC$ followed by *RhoGAP* and *RhoA* then the output $p-SRC$ to reach stability (Figures 2 and Figure 4). For Case 1 MLC reaches a plateau.

For the purpose of validation, we also tested a negative proof for the model, where we considered ECM-INT0=0, which is equivalent to a null focal adhesion signal. In this scenario, all the other parameters were maintained constant and it resulted in a flat distribution and no interaction was observed in the system (data not shown).

In Figure 5 results for perturbations are shown. We take into account one perturbation at a time. In Figure 5a(i) we simulate the Case 2 in Tables 3 and 4. This case shows the effects to take $k_{EF^p} = 1$ ten times greater than the reference in Case 1. It is equivalent to saying that the *FAK* would be more activated than SRC from the extracellular signal. Comparing Figure 5a(i) with Figure 4b(i), we can see that the concentration of $p-FAK$ is great for case 2 and also that the concentration of $p-SRC$ is reduced. The results for the output protein MLC and $p-SRC$ are shown in Figure 5(b)(i). For case 2 it also reached a plateau.

In Figure 5a(ii) we simulate the Case 3 in Tables 3 and 4. In this case, we increased the initial concentration of $FAK_0 = 20$. The behavior of the proteins $p-FAK$ and $p-SRC$ are not distinguishable from case 1 (Figures 5a(ii) and 4). But the behavior of MLC changes, we can see that $p-SRC$ starts to oscillate around a mean value and it is not a smooth plateau anymore.

In Figure 5a(iii) we simulate the Case 4 in Tables 3 and 4. In this case, we increased the rate of interaction of SRC, $k_{ES^p} = 1$. The concentration of the protein $p-FAK$ decreases with respect to case 1 (Figures 5a(iii) and 4). We can see that the amplitude of the oscillations of $p-SRC$ decrease in relation to those in case 3 (Figure 5b(ii)). Finally, in Figure 5a(iv) we simulate the Case 5 in Tables 3 and 4. In this case, we increased the initial concentration of $SRC_0 = 20$. The concentrations of $p-FAK$ and $p-SRC$ are not distinguishable from case 1 (Figures 5a(iv) and 4). We can see that the amplitude of the oscillations of $p-SRC$ have the same range as in case 3 (Figure 5b(ii)).

doi: 10.58560/rmmsb.v03.n02.023.04

Table 2: List of generation and recombination terms used to build the stochastic model using the chemical master equation.

Protein	Chemical Master equation term
$p-FAK$	$g([p-FAK],t) = \frac{k_{EF^p}([ECMINT]-[p-MLC])[FAK]}{k_1+[FAK]} + \frac{k_{FF^p}[FAK][p-FAK]}{k_3+[p-FAK]} + \frac{k_{S^pF^p}[p-SRC][FAK]}{k_7+[FAK]}$
$p-FAK$	$r([p-FAK],t) = k_{F^pF}[p-FAK] + \frac{k_{F^pS^p}[p-FAK][SRC]}{k_4+[SRC]} + \frac{k_{F^pRhoGEF}[p-FAK][RhoGEF]}{k_8+[RhoGEF]}$
$p-SRC$	$g([p-SRC],t) = \frac{k_{ES^p}([ECMINT]-[p-MLC])[SRC]}{k_2+[SRC]} + \frac{k_{F^pS^p}[p-FAK][SRC]}{k_4+[SRC]} + \frac{k_{SSP}[SRC][p-SRC]}{k_6+[p-SRC]}$
$p-SRC$	$r([p-SRC],t) = k_{S^pS}[p-SRC] + \frac{k_{S^pF^p}[p-SRC][FAK]}{k_7+[FAK]} + \frac{k_{S^pRhoGAP}[p-SRC][RhoGAP]}{K_9+[RhoGAP]}$
$RhoGEF$	$g([RhoGEF],t) = \frac{k_{F^pRhoGEF}[p-FAK][RhoGEF]}{k_8+[RhoGEF]}$
$RhoGEF$	$r([RhoGEF],t) = \frac{k_{RhoGEFRhoA}[RhoGEF][RhoA]}{k_{11}+[RhoA]}$
$RhoGAP$	$g([RhoGAP],t) = \frac{k_{S^pRhoGAP}[p-SRC][RhoGAP]}{K_9+[RhoGAP]}$
$RhoGAP$	$r([RhoGAP],t) = \frac{k_{RhoGAPRhoA}[RhoGAP][RhoA]}{k_{11}+[RhoA]}$
$RhoA$	$g([RhoA],t) = \frac{k_{RhoGEFRhoA}[RhoGEF][RhoA]}{k_{10}+[RhoA]}$
$RhoA$	$r([RhoA],t) = \frac{k_{RhoGAPRhoA}[RhoGAP][RhoA]}{k_{11}+[RhoA]}$
$p-MLC$	$g([p-MLC],t) = \frac{k_{RHOAMLC^p}[RhoA][MLC]}{k_{12}+[MLC]} + \frac{k_{MLCPMLC^p}[MLC][p-MLC]}{k_{13}+[MLC]}$
MLC^p	$r([p-MLC],t) = k_{MLC^pMLC}[p-MLC]$

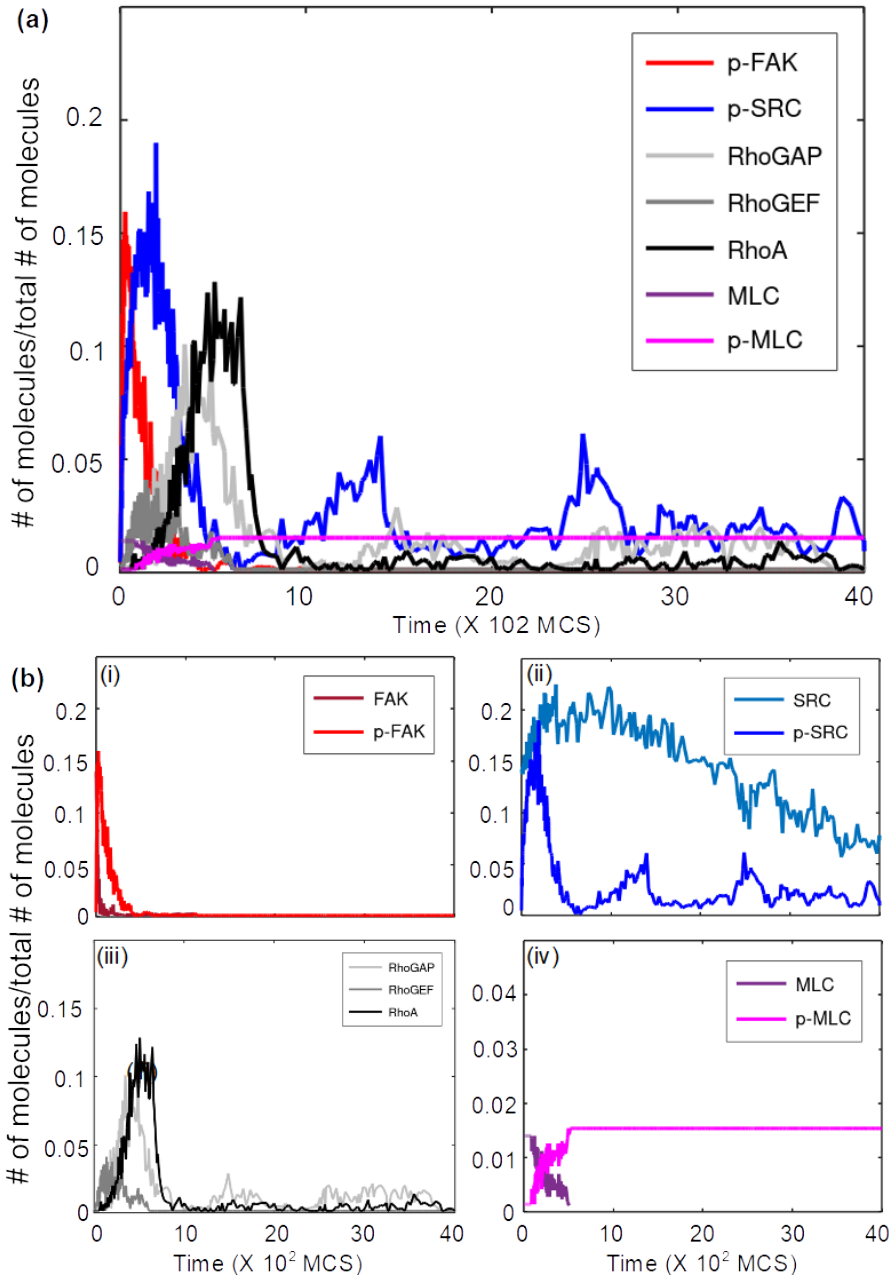

Figure 4: Normalized distribution of proteins per Monte Carlo step (MCS). (a) Dynamic activation of key signaling proteins of the base network. (b) The detailed dynamic of each circuit in the network: (i) FAK (ii) SCR (iii) Rho family and (iv) MLC was zoomed-in protein concentration, for a max concentration of 0.05. All the plots show the mean of 10 simulations. For visualization purposes, each point represents the mean of the concentration for 10-time steps. The parameters used for these simulations are detailed in Tables 3 and 4.

doi: 10.58560/rmmsb.v03.n02.023.04

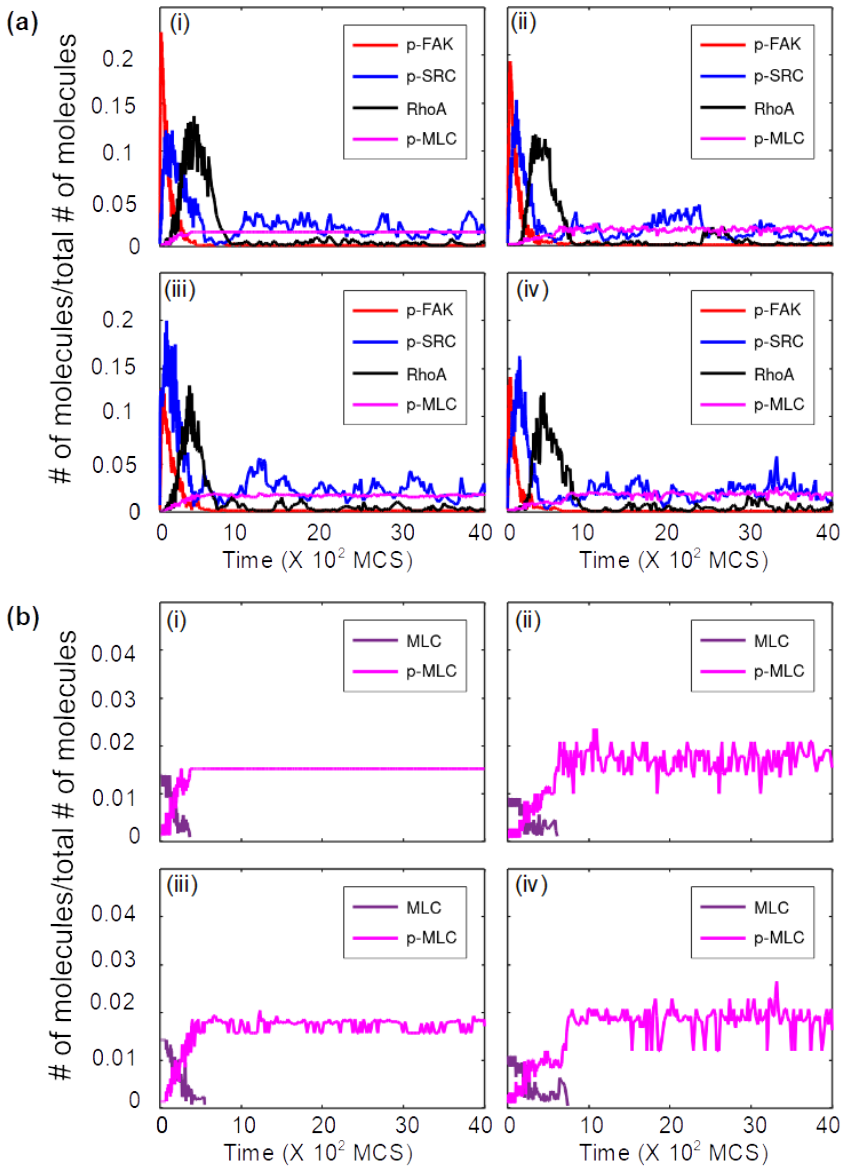

Figure 5: Comparison of the perturbations made in the parameters of the model. (a) The concentration of the key proteins in the system ($p-FAK$, $p-SRC$, $RhoA$ and $p-MLC$) the figures show only the initial 400 MCS for the purpose to see how the early proteins are behaving. (b) The concentration of proteins for the output MLC and $p-MLC$. The subdivision of the figures are (i) Case 2; (ii) Case 3; (iii) Case 4 (iv) Case 5. The parameters used for these simulations are detailed in Tables 3 and 4.

doi: 10.58560/rmmsb.v03.n02.023.04

4 DISCUSSION

We proposed a stochastic mathematical model using the solution of the Chemical Master equation to understand the network of proteins involving extracellular matrix stimuli that can lead to actin polymerization and focal adhesion formation. Our signaling network was built considering the interaction between the focal adhesion proteins *FAK*, Src, Rac, Rho, Myosin light-chain (*MLC*) (Figures 1 and 2). Our data showed the capacity of the model to predict expected behaviors by reproducing a cascade of events and dependence on the activation of proteins of a known signaling pathway, as follows.

Our results have shown that *FAK* activity is lower than Src activity (see figures 4 and 5), which confirms what was experimentally observed by Caron-Lormier and Berry Caron-Lormier and Berry (2005). Furthermore, we observed that the increase of activation rate of $p-FAK$ (Case 2, Figure 5a(i)) did not influence the dynamic of other proteins, only the initial concentration of $p-FAK$. A behavior that was observed experimentally by Stutchbury et. al Stutchbury *et al.* (2017).

For cases 3, 4, and 5 oscillations in the dynamics of $p-MLC$ were observed (Figures 5b (ii), (iii) and (iv)). These oscillations are more evident in the cases we are varying the initial concentration of *FAK* and SRC (Figures 5b (ii), and (iv), respectively). Which can be associated with a stiff substrate and higher protein recruitment to the focal adhesion. Stutchbury et. al Stutchbury *et al.* (2017) showed that a modular composition of FAs with the mobile behavior of protein subsets responded differently when encountering environments of different rigidities.

In summary, we proposed a stochastic model considering the dynamic of focal adhesion proteins leading to actin polymerization. Our model was built in a combination of experimental and theoretical observations and was able to demonstrate a variety of behaviors for the different proteins and circuits within the network. Furthermore, we showed the effect of variation in the parameters that can lead to different cell fates.

SUPPORT

Research partially supported by:

- National Council for Scientific and Technological Development (CNPQ), Ministry of Science and Technology, Brazil. PIBIC No. 21-2022 Process 107099-2023-3 (2023). *Programa Institucional de Bolsas de Iniciação Científica*
- Fundação de Amparo à Pesquisa do Estado do Rio Grande do Sul, Brazil. PROA 23-25551-0001199-9 (2023). *Network of interaction of proteins. Decision between apoptosis and senescence*.

CONTRIBUTION OF THE AUTHORS (CREDIT)

Conceptualization: Luciana Renata de Oliveira
Data curation: Luciana Renata de Oliveira, Júlia Vitória Ribeiro, Alícia Groth Becker, Gabriel Vitorello, José Carlos Merino Mombach.
Investigation: Luciana Renata de Oliveira, Júlia Vitória Ribeiro, Alícia Groth Becker, Gabriel Vitorello
Writing – original draft: Luciana Renata de Oliveira and José Carlos Merino Mombach.

APPENDIX

A LIST OF EQUATIONS FOR EACH INTERACTION

The list of equations for each reaction represented in Figure 2. The indexes correspond to those in Figure 2, the equation and the kind of reaction are also represented in the table.

B PARAMETERS FOR THE SIMULATIONS

The list of equations for each reaction represented in Figure 2. The indexes correspond to those in Figure 2, the equation and the kind of reaction are also represented in the table.

Table 3: List of equations for each reaction represented in Figure 2. The indexes correspond to those in Figure 2, the equation and the kind of reaction are also represented in the table.

Index	Reaction	Equation	Reaction kind
1	$ECMINT \to p-FAK$	$\frac{k_{EFP}([ECMINT]-[p-MLC])[FAK]}{k_1+[FAK]}$	Michaelis-Menten
2	$ECMINT \to p-SRC$	$\frac{k_{ESP}([ECMINT]-[p-MLC])[SRC]}{k_2+[SRC]}$	Michaelis-Menten
3	$FAK \to p-FAK$	$\frac{k_{FFP}[FAK][p-FAK]}{k_3+[p-FAK]}$	Michaelis-Menten
4	$p-FAK \to p-SRC$	$\frac{k_{FPSP}[p-FAK][SRC]}{k_4+[SRC]}$	Michaelis-Menten
5	$SRC \to p-SRC$	$\frac{k_{SSP}[SRC][p-SRC]}{k_6+[p-SRC]}$	Michaelis-Menten
6	$p-FAK \to FAK$	$k_{FPF}[p-FAK]$	Degradation
7	$p-SRC \to p-FAK$	$\frac{k_{SPFP}[p-SRC][FAK]}{k_7+[FAK]}$	Michaelis-Menten
8	$p-SRC \to SRC$	$k_{SPS}[p-SRC]$	Degradation
9	$p-FAK \to RHOGEF$	$\frac{k_{FPRhoGEF}[p-FAK][RhoGEF]}{k_8+[RhoGEF]}$	Michaelis-Menten
10	$p-SRC \to RHOGAP$	$\frac{k_{SPRhoGAP}[p-SRC][RhoGAP]}{k_9+[RhoGAP]}$	Michaelis-Menten
11	$RHOGEF \to RHOA$	$\frac{k_{RhoGEFRhoA}[RhoGEF][RhoA]}{k_{10}+[RhoA]}$	Michaelis-Menten
12	$RHOGAP \dashv RHOA$	$\frac{k_{RhoGAPRhoA}[RhoGAP][RhoA]}{k_{11}+[RhoA]}$	Inhibition
13	$RHOA \dashv p-MLC$	$\frac{k_{RHOAMLCP}[RhoA][MLC]}{k_{12}+[MLC]}$	Michaelis-Menten
14	$MLC \to p-MLC$	$\frac{k_{MLCPMLCP}[MLC][p-MLC]}{k_{13}+[MLC]}$	Michaelis-Menten
15	$p-MLC \to MLC$	$k_{MLCPMLC}[p-MLC]$	Degradation

Table 4: List of equations for each reaction represented in Figure 2. The indexes correspond to those in Figure 2, the equation and the kind of reaction are also represented in the table.

Rate($/s$)	Case 1	Case 2	Case 3	Case 4	Case 5
1	$ECMINT \to p-FAK$	$\frac{k_{EFP}([ECMINT]-[p-MLC])[FAK]}{k_1+[FAK]}$	Michaelis-Menten		
2	$ECMINT \to p-SRC$	$\frac{k_{ESP}([ECMINT]-[p-MLC])[SRC]}{k_2+[SRC]}$	Michaelis-Menten		
3	$FAK \to p-FAK$	$\frac{k_{FFP}[FAK][p-FAK]}{k_3+[p-FAK]}$	Michaelis-Menten		
4	$p-FAK \to p-SRC$	$\frac{k_{FPSP}[p-FAK][SRC]}{k_4+[SRC]}$	Michaelis-Menten		
5	$SRC \to p-SRC$	$\frac{k_{SSP}[SRC][p-SRC]}{k_6+[p-SRC]}$	Michaelis-Menten		
6	$p-FAK \to FAK$	$k_{FPF}[p-FAK]$	Degradation		
7	$p-SRC \to p-FAK$	$\frac{k_{SPFP}[p-SRC][FAK]}{k_7+[FAK]}$	Michaelis-Menten		
8	$p-SRC \to SRC$	$k_{SPS}[p-SRC]$	Degradation		
9	$p-FAK \to RHOGEF$	$\frac{k_{FPRhoGEF}[p-FAK][RhoGEF]}{k_8+[RhoGEF]}$	Michaelis-Menten		
10	$p-SRC \to RHOGAP$	$\frac{k_{SPRhoGAP}[p-SRC][RhoGAP]}{k_9+[RhoGAP]}$	Michaelis-Menten		
11	$RHOGEF \to RHOA$	$\frac{k_{RhoGEFRhoA}[RhoGEF][RhoA]}{k_{10}+[RhoA]}$	Michaelis-Menten		
12	$RHOGAP \dashv RHOA$	$\frac{k_{RhoGAPRhoA}[RhoGAP][RhoA]}{k_{11}+[RhoA]}$	Inhibition		
13	$RHOA \dashv p-MLC$	$\frac{k_{RHOAMLCP}[RhoA][MLC]}{k_{12}+[MLC]}$	Michaelis-Menten		
14	$MLC \to p-MLC$	$\frac{k_{MLCPMLCP}[MLC][p-MLC]}{k_{13}+[MLC]}$	Michaelis-Menten		
15	$p-MLC \to MLC$	$k_{MLCPMLC}[p-MLC]$	Degradation		

REFERENCES

Aguda, B. and Friedman, A. (2008) *Models of cellular regulation*. Oxford University Press.

Atherton, P., Stutchbury, B., Jethwa, D. and Ballestrem, C. (2016) 'Mechanosensitive components of integrin adhesions: Role of vinculin'. *Experimental cell research*, 343(1), pp. 21–27.

Berro, J. (2018) '"essentially, all models are wrong, but some are useful"—a cross-disciplinary agenda for building useful models in cell biology and biophysics'. *Biophysical Reviews*, 10(6), pp. 1637–1647.

Calderwood, D.A., Campbell, I.D. and Critchley, D.R. (2013) 'Talins and kindlins: partners in integrin-mediated adhesion'. *Nature reviews Molecular cell biology*, 14(8), pp. 503–517.

Carisey, A., Tsang, R., Greiner, A.M., Nijenhuis, N., Heath, N., Nazgiewicz, A., Kemkemer, R., Derby, B., Spatz, J. and Ballestrem, C. (2013) 'Vinculin regulates the recruitment and release of core focal adhesion proteins in a force-dependent manner'. *Current biology*, 23(4), pp. 271–281.

Caron-Lormier, G. and Berry, H. (2005) 'Amplification and oscillations in the fak/src kinase system during integrin signaling'. *Journal of theoretical biology*, 232(2), pp. 235–248.

Chen, H., Choudhury, D.M. and Craig, S.W. (2006) 'Coincidence of actin filaments and talin is required to activate vinculin'. *Journal of Biological Chemistry*, 281(52), pp. 40389–40398.

Dai, Y., Luo, W. and Chang, J. (2018) 'Rho kinase signaling and cardiac physiology'. *Current opinion in physiology*, 1, pp. 14–20.

De Oliveira, L.R. (2014) 'Master equation: Biological applications and thermodynamic description'.

Del Rio, A., Perez-Jimenez, R., Liu, R., Roca-Cusachs, P., Fernandez, J.M. and Sheetz, M.P. (2009) 'Stretching single talin rod molecules activates vinculin binding'. *Science*, 323(5914), pp. 638–641.

Giampieri, E., Remondini, D., De Oliveira, L., Castellani, G. and Lió, P. (2011) 'Stochastic analysis of a mirna–protein toggle switch'. *Molecular BioSystems*, 7(10), pp. 2796–2803.

Gillespie, D.T. (1977) 'Exact stochastic simulation of coupled chemical reactions'. *The journal of physical chemistry*, 81(25), pp. 2340–2361.

Hirata, H., Chiam, K.H., Lim, C.T. and Sokabe, M. (2014) 'Actin flow and talin dynamics govern rigidity sensing in actin–integrin linkage through talin extension'. *Journal of The Royal Society Interface*, 11(99), p. 20140734.

Hsia, D.A., Mitra, S.K., Hauck, C.R., Streblow, D.N., Nelson, J.A., Ilic, D., Huang, S., Li, E., Nemerow, G.R., Leng, J. *et al.* (2003) 'Differential regulation of cell motility and invasion by fak'. *The Journal of cell biology*, 160(5), pp. 753–767.

Jansen, K., Atherton, P. and Ballestrem, C. (2017) 'Mechanotransduction at the cell-matrix interface'. In *Seminars in cell & developmental biology*, vol. 71. Elsevier, pp. 75–83.

Jaqaman, K., Loerke, D., Mettlen, M., Kuwata, H., Grinstein, S., Schmid, S.L. and Danuser, G. (2008) 'Robust single-particle tracking in live-cell time-lapse sequences'. *Nature methods*, 5(8), pp. 695–702.

Kanchanawong, P., Shtengel, G., Pasapera, A.M., Ramko, E.B., Davidson, M.W., Hess, H.F. and Waterman, C.M. (2010) 'Nanoscale architecture of integrin-based cell adhesions'. *Nature*, 468(7323), pp. 580–584.

Kumar, A., Ouyang, M., Van den Dries, K., McGhee, E.J., Tanaka, K., Anderson, M.D., Groisman, A., Goult, B.T., Anderson, K.I. and Schwartz, M.A. (2016) 'Talin tension sensor reveals novel features of focal adhesion force transmission and mechanosensitivity'. *Journal of Cell Biology*, 213(3), pp. 371–383.

Lessey, E.C., Guilluy, C. and Burridge, K. (2012) 'From mechanical force to rhoa activation'. *Biochemistry*, 51(38), pp. 7420–7432.

Lippincott-Schwartz, J., Snapp, E.L. and Phair, R.D. (2018) 'The development and enhancement of frap as a key tool for investigating protein dynamics'. *Biophysical journal*, 115(7), pp. 1146–1155.

MacKay, C.E. and Knock, G.A. (2015) 'Control of vascular smooth muscle function by src-family kinases and reactive oxygen species in health and disease'. *The Journal of physiology*, 593(17), pp. 3815–3828.

Martin-Camara, O., Cores, A., Lopez-Alvarado, P. and Menéndez, J.C. (2021) 'Emerging targets in drug discovery against neurodegenerative diseases: Control of synapsis disfunction by the rhoa/rock pathway'. *European Journal of Medicinal Chemistry*, 225, p. 113742.

Nagano, M., Hoshino, D., Koshikawa, N., Akizawa, T., Seiki, M. *et al.* (2012) 'Turnover of focal adhesions and cancer cell migration'. *International journal of cell biology*, 2012.

de Oliveira, L.R. and Jaqaman, K. (2019) 'Fisik: Framework for the inference of in situ interaction kinetics from single-molecule imaging data'. *Biophysical journal*, 117(6), pp. 1012–1028.

Pertz, O. (2010) 'Spatio-temporal rho gtpase signaling–where are we now?' *Journal of cell science*, 123(11), pp. 1841–1850.

Raaijmakers, J.G. (1987) 'Statistical analysis of the michaelis-menten equation'. *Biometrics*, pp. 793–803.

Roca-Cusachs, P., Del Rio, A., Puklin-Faucher, E., Gauthier, N.C., Biais, N. and Sheetz, M.P. (2013) 'Integrin-dependent force transmission to the extracellular matrix by α-actinin triggers adhesion maturation'. *Proceedings of the National Academy of Sciences*, 110(15), pp. E1361–E1370.

Soriano, O., Alcón-Pérez, M., Vicente-Manzanares, M. and Castellano, E. (2021) 'The crossroads between ras and rho signaling pathways in cellular transformation, motility and contraction'. *Genes*, 12(6), p. 819.

Srinivasan, B. (2022) 'A guide to the michaelis–menten equation: steady state and beyond'. *The FEBS journal*, 289(20), pp. 6086–6098.

Stutchbury, B., Atherton, P., Tsang, R., Wang, D.Y. and Ballestrem, C. (2017) 'Distinct focal adhesion protein modules control different aspects of mechanotransduction'. *Journal of cell science*, 130(9), pp. 1612–1624.

Szklarczyk, D., Gable, A.L., Lyon, D., Junge, A., Wyder, S., Huerta-Cepas, J., Simonovic, M., Doncheva, N.T., Morris, J.H., Bork, P. *et al.* (2019) 'String v11: protein–protein association networks with increased coverage, supporting functional discovery in genome-wide experimental datasets'. *Nucleic acids research*, 47(D1), pp. D607–D613.

Valencia-Expósito, A., Grosheva, I., Míguez, D.G., González-Reyes, A. and Martín-Bermudo, M.D. (2016) 'Myosin light-chain phosphatase regulates basal actomyosin oscillations during morphogenesis'. *Nature communications*, 7(1), p. 10746.

Van Kampen, N.G. (1992) *Stochastic processes in physics and chemistry*, vol. 1. Elsevier.

Recommended Citation: Renata de Oliveira, L. *et al.* (2023). *'Using the Chemical Master Equation to model the interaction network of focal adhesion proteins'*. Rev. model. mat. sist. biol. 3(E), e23R05, doi:10.58560/rmmsb.v03.n02.023.04

Support: PIBIC No. 21-2022, PROA 23-25551-0001199-9 (2023)